

https://dspace.org/

The dynamics of mine hoist catenaries

Constancon, Charles Peter

2011-04-20
http://hdl.handle.net/10539/9610

Downloaded from a DSpace repository. https://dspace.org/

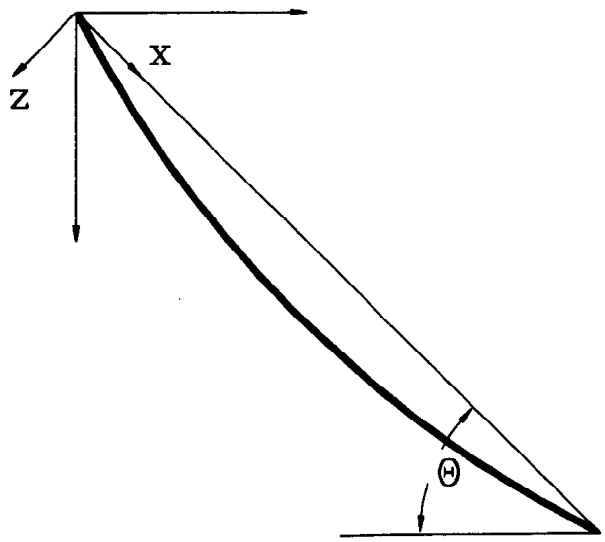


Figure 3.6: Flat sag inclined cable

to $\lambda^2 = (mglcos(\theta)/H)/(HL_e/EA)$. Perkins and Mote[1987] demonstrated that the loss of symmetry of the profile of an inclined cable, leads to frequency veering as opposed to coalescence in the proximity of a modal cross-over.

In the context of mine hoist systems, the cable tension is sufficiently high such that the assumption of a flat sag cable profile symmetrical with respect to the span is reasonable[8]. Mankowski[1982] introduced this approximation by treating the catenary as being horizontally supported, symmetric with respect to the mid-span, and correcting the gravitational constant to $gcos(\theta)$. Although the equations derived account correctly for the tension and curvature distribution in the catenary, this approximation will be introduced, and consequently the system analysed is presented in figure 3.7.

Considering the equations of static equilibrium of the catenary, the variation of tension along the cable due to its self weight is negligible, and the cable tension and curvature are constant. Thus $P^i, s \approx 0$, c^i is constant and $l_t \approx 0$ and $l_n \approx 1$. Equation 3.4 is trivial, whilst equation 3.5 results in a description of the equilibrium curvature where g has been corrected to $gcos(\theta)$. Applying these approximations to equations 3.4,3.5 results in:

$$P^i(s) = P^i$$

[8]In typical mine hoist systems, $0.01 < \epsilon < 0.05$, $\lambda^2 < 2$

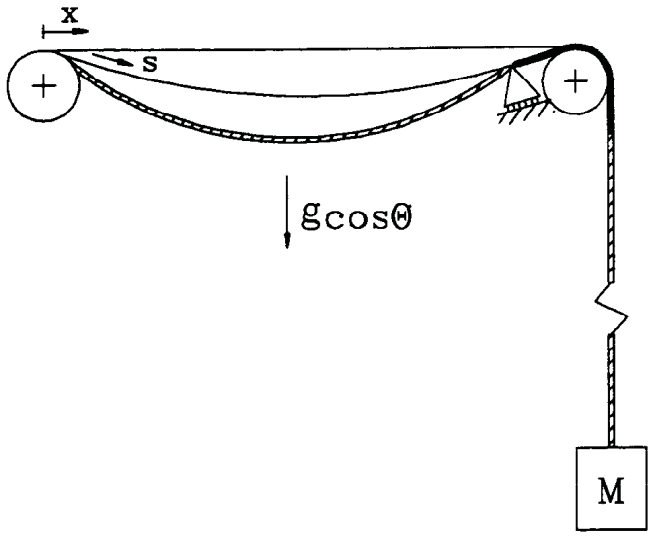


Figure 3.7: Mine hoist model

$$\kappa = \frac{\rho A^i g cos\theta}{P^i - \rho A^i (c^i)^2}$$

Equations 3.6-3.8 define the static tension distribution in the rope, which give:

$$\overline{P}^i(l_c) = P^i = Mg + \rho A^i[(c^i)^2 + l_v g]$$

Thus the equilibrium curvature of the catenary is determined by:

$$\kappa = \frac{\rho A^i cos\theta}{M + \rho A^i l_v}$$

The equilibrium profile is defined by:

$$\mathbf{z} = \frac{1}{2}\mathbf{x}(1 - \mathbf{x})$$

where $\mathbf{z} = z/(mgl^2 cos(\theta)/H)$, $\mathbf{x} = x/l$; z represents the perpendicular distance between the profile and the chord, x represents the distance along the chord between the drum and sheave.

The equations of motion are simplified further by treating $u = O(v^2) = O(w^2)$, and retaining terms up to $O(v^3), O(w^3)$, and terms to $O(v^2), O(w^2)$ which have curvature κ as a coefficient[9]. Thus the equations of motion applied to analyse the mine hoist system are defined as:

$$u_{,tt} + 2c^i u_{t,s} - c^i\kappa\{v_{,t} + 2c^i v_{,s} + c^i\kappa u\} + c^i_{,t}\{1 + u_{,s} - \kappa v\} = (c_l^2 - c^{i^2})u_{,ss} + c_l^2\{v_{,s}v_{,ss} + w_{,s}w_{,ss} - \kappa v_{,s}\} \tag{3.9}$$

$$v_{,tt} + 2c^i v_{t,s} - c^i\kappa\{u_{,t} - c^i\kappa v\} + c^i_{,t}\{v_{,s} + \kappa u\} = (c_v^2 - c^{i^2})v_{,ss} + c_l^2\{(u_{,s}v_{,s})_{,s} + \frac{3}{2}v_{,s}^2 v_{,ss} + \frac{1}{2}w_{,s}^2 v_{,ss} + v_{,s}w_{,s}w_{,ss}\} - \kappa c_l^2\{vv_{,ss} - u_{,s} + \kappa v + \frac{1}{2}v_{,s}^2 - \frac{1}{2}w_{,s}^2\} \tag{3.10}$$

$$w_{,tt} + 2c^i w_{t,s} + c^i_{,t}w_{,s} = (c_v^2 - c^{i^2})w_{,ss} + c_l^2\{(u_{,s}w_{,s})_{,s} + \frac{3}{2}w_{,s}^2 w_{,ss} + \frac{1}{2}v_{,s}^2 w_{,ss} + w_{,s}v_{,s}v_{,ss}\} - \kappa c_l^2\{vw_{,ss} + w_{,s}v_{,s}\} \tag{3.11}$$

$$\overline{u}_{,tt} + 2c^i\overline{u}_{t,s} + c^i_{,t}\{1 + \overline{u}_{,s}\} = (c_l^2 - c^{i^2})\overline{u}_{,ss}$$

$$\left[A^i E\{\overline{\epsilon} - \epsilon a_1\}\right]|_{l_c} - \rho A^i (c^i)^2(\overline{u}_{,s} - u_{,s})|_{l_c} = [\frac{I}{R^2}(\dot{u}_1 + c^i)]_{,t}$$

$$-[A^i E\overline{\epsilon}]|_{l_v} = [M(\dot{u}_2 + c^i)]_t - \rho A^i c^i \dot{u}_2$$

where $c_l = E/\rho$, $c_v = P^i/\rho A^i$, represent the longitudinal and lateral wave speed respectively. c^i, c^i_t represent the transport velocity and acceleration of the rope respectively.

[9]The same equations result if the strain measure is defined as: $\epsilon = u_{,s} - \kappa v + \frac{1}{2}(v_{,s}^2 + w_{,s}^2)$

The displacements u, v, w are referenced to the local tangential, normal and bi-normal directions of the catenary profile respectively. In the limit where $\kappa \doteq 0$, the unit vectors $\underline{t}^i, \underline{n}^i, \underline{b}^i$ align with the cartesian unit vectors $\underline{e}_1, \underline{e}_2, \underline{e}_3$, and the arc length co-ordinate s is replaced by the cord length co-ordinate x. The displacements in the cartesian plane u_c, v_c, w_c may be found by applying a transformation of axes $u_c = u + z_x v, v_c = v, - z_x u, w_c = w$[10].

3.4 Conclusion

This chapter has developed the equations of motion applicable to the mine hoist system. However, further development is required to account for the excitation mechanism. In this regard, the excitation can be defined broadly as comprising of inertial loading of the system due to the acceleration/deceleration profile employed to accelerate the system to, or decelerate the system from the nominal winding velocity, and periodic boundary excitation at the drum due to the coil cross-over mechanism. The latter excitation comprises of periodic pulses normal, transverse and tangential to the drum radius. Once the rope has traversed the full drum width, a layer change occurs, which induces a significant axial and radial pulse to the rope at the drum end. Following the layer change, the traverse direction of the rope changes, and consequently the lateral component of the periodic excitation due to the coil cross-over profile changes phase by 180°. To complicate matters further, during the wind the system parameters are changing due to the decreasing or increasing length of the suspended vertical cable. Thus both the system parameters and the excitation are strictly non-stationary. This aspect introduces a substantial complication to a purely theoretical analysis of the system. Mankowski[1982] appreciated that a theoretical analysis of the system, which accounted for the complex excitation induced by the coil cross-over, as well as the nonlinear nature of the system would lead to a situation intractable to analysis, and thus proposed a numerical analysis of the system. Although ultimately a numerical simulation of the system would be essential, in the current study where the equations of motion have been developed, it is possible to examine the stationary nature of the system to stationary periodic excitation at the drum, prior to a numerical simulation. Achieving desirable stationary system characteristics would extend the current linear design approach, thus providing an initial selection of

[10]The equations of motion could have been derived to reflect displacements in a cartesian reference frame directly (Luogno et al [1984]), however it was decided to use a Lagrangian reference, since it results in a more concise presentation for the general equations. The strain measure applied by Luogno et al[1984], $\epsilon = u_{,x} + y_{,x} v_{,x} + \frac{1}{2} v_{,x}^2$ can be obtained by applying the co-ordinate transformations $u_c = u + z_x v, v_c = v - z_x u$ to the equivalent strain measure $\epsilon = u_{,s} - kv + \frac{1}{2} v_{,s}^2$ in the Lagrangian reference frame, and ordering terms appropriately.

system parameters for assessment in a numerical simulation. Since the excitation definition is dependent on whether a stationary or nonstationary analysis is pursued, it will be presented where appropriate in later chapters.

Chapter 4

Stationary Analysis of the Mine Hoist System

The purpose of this study is to identify conditions leading to, or promoting the occurrence of rope whip on mine hoist systems. Although the analysis of the large non-linear motion the system may present a challenging problem, it is not the initial focus of this study. Ideally, the analysis of the system should evolve in a consistent manner, supporting further more complex studies. This philosophy has been applied, where the current analysis of the mine hoist system consists of two phases. This chapter considers the first phase, which examines the steady state behaviour of the system in the absence of rope curvature and transport velocity. The rationale of this phase grows from the approach presented by Dimitriou and Whillier[1973], where the linear natural frequencies of the system were examined as a function of the shaft depth. Dimitriou and Whillier[1973] proposed their quasi-static linear analysis to identify regions where primary external resonance of the system could be expected. This analysis did not provide information regarding the severity of the interaction of the longitudinal and lateral modes, and hence the significance of the system tuning. Since the lateral excitation induced by the Lebus coiling motion is more significant than the longitudinal excitation, it is usual to attempt to avoid lateral catenary resonance, whilst neglecting the longitudinal system behaviour. This strategy is often not successful, particularly with respect to deep shafts. In fact it would be unusual to find a mine hoist system in practice, where primary external resonance of the system does not occur at some stage during the ascending or descending cycle. Although catenary resonance generally occurs, some systems exhibit more severe behaviour than others. This supports the notion that the overall system tuning may be an important feature influencing the system behaviour. This is a pertinent observation, since it is possible for

the lateral catenary motion to induce autoparametric system response due to the non-linear coupling between the lateral and longitudinal modes. Dimitriou and Whillier[1973] discussed this possibility qualitatively, and proposed that an autoparametric excitation mechanism was probably responsible for the observed lateral motion of the vertical section of the rope. Although the results presented by Dimitriou and Whillier[1973] provide a basis for a qualitative discussion, in practice they are only useful to define conditions of primary external resonance of the system. In order for an analysis to be practical, a quantitative analysis, accounting for the degree of excitation, damping, and the system tuning is required.

In the context of Industry, such an analysis should present the results in an unambiguous and simple manner. Ideally the analysis should identify regions of avoidance regarding the system parameters, rather than presenting the design engineer with a thorough non-linear steady state solution of the modal amplitudes, which may be multi-valued and even non-periodic. Linear dynamic characteristics of a system are generally well understood by graduate engineers, however this is not the case with regard to non-linear studies. It is for this reason that the concept of avoidance of non-linear interaction is proposed as a basis for assessing the dynamic behaviour of the system. Thus the method presented considers the avoidance of significant non-linear behaviour as a criterion for designing a mine hoist system. This criterion is based on the formulation of a datum steady state solution. The datum solution is chosen as the *linear* solution in the absence of primary external resonance.

Regions of non-linear interaction, where the response will deviate from the datum solution due to non-linear effects are identified by considering the stability of the motion in the context of the non-linear equations of motion. The linear stability analysis is defined by considering the stability of a system of equations with periodic coefficients, and consequently regions of avoidance are identified by constructing a stability chart which is synonymous with the Strutt stability chart. This represents the first phase of the analysis, where system parameters satisfying this criterion are selected. The non-stationary nature of the system, as well as transient excitation induced during a layer change requires a more advanced analysis. Chapter 5 presents a complete non-linear numerical simulation of the system, which accounts for the non-stationary system characteristics, transient excitations, rope curvature and winding velocity.

4.1 The Steady State Analysis

The non-linear equations of motion of the system developed in Chapter 3, are considered in the absence of catenary curvature and axial transport velocity. Initially, the lateral stability of the catenary was investigated under the influence of stationary periodic axial excitation. In this case the trivial condition $v(s,t) = w(s,t) = 0$ for the lateral motion represents a possible solution, where non-trivial lateral motion results as a consequence of dynamic instability. By applying the trivial condition, $v(s,t) = w(s,t) = 0$, to the equations of motion, an independent linear wave equation describes the forced steady state longitudinal system response. This equation can be solved in closed form. Conversely the non-linear lateral equations of motion represent variational equations, which describe the stability of the trivial state of the lateral modes to small disturbances. Since the longitudinal steady state response may be defined in closed form, terms which couple the lateral variational equations to the longitudinal motion may be eliminated by direct substitution. Consequently the linear stability of the lateral variational modes is described by a set of Hill type equations with periodic coefficients. This analysis is presented in detail in Appendix B, where a perturbation technique and a harmonic balance method are applied to define regions of linear instability of the trivial lateral motion of the catenary to small disturbances. The stability analysis confirms that the lateral stability of the trivial state of the catenary is disrupted when conditions of simple and additive combination parametric resonance arise. Such conditions are related to the proximity of the axial excitation frequency to a condition of parametric resonance, and the amplitude of the parametric excitation, which is governed by the steady state longitudinal motion. Although the longitudinal excitation is small, this motion is amplified at longitudinal resonance, enhancing regions of lateral instability. Consequently narrow regions of parametric instability may result when the system is tuned to a condition of longitudinal resonance, even when the system is not closely tuned to a parametric resonance. The amplitude of the forced longitudinal response is sensitive to dissipation, and consequently these regions are quickly eroded by the inclusion of longitudinal damping.

Since the external longitudinal excitation of the system is small in comparison to the lateral excitation, the longitudinal response induced by the forced lateral motion is significant. Accounting for the lateral motion enhances the autoparametric nature of the system, whereby lateral catenary motion causes forced longitudinal system response. Autoparametric response is enhanced when the system tunes to an internal resonance, for instance where a longitudinal mode is tuned to twice the frequency of the lateral mode. In such a case, lateral motion may induce significant longitudinal reponse. In addi-

tion, due to the coupling between the lateral and longitudinal motion, regions of secondary resonance may arise when the excitation tunes to additive and difference combinations of the longitudinal and lateral modes.

As the most significant excitation to the system occurs axially, and in the out-of-plane lateral direction parallel to the winder drum surface, in-plane excitation and consequently in-plane response due to the drum excitation is assumed negligible. In the absence of catenary curvature direct excitation of lateral in-plane motion, due to curvature coupling with the longitudinal motion does not arise. Products coupling the in-plane and longitudinal motion exist in the in-plane equation of motion, thus the in-plane modes are parametrically excited, and consequently non-trivial response arises through instability or bifurcation. Thus the *linear* steady state out-of-plane response due to longitudinal and lateral out-of-plane excitation forms the basis for constructing a datum solution. Three dimensional motion, or rope whip followed by further intermodal energy exchanges between the longitudinal and lateral modes is initiated as a consequence of bifurcation of the planar steady state motion.

Longitudinal and lateral damping is accounted for in the steady state datum solution. The particular form of the damping model assumed is of significance, particularly with regard to the longitudinal response. In the past, Industry has assumed that a relative proportional viscous damping mechanism[1] applied to the longitudinal dissipation. Rudimentary tests performed by industry (Thomas et al.[1987], Greenway[1989]) approximate the dimensionless modal damping ratio of the fundamental longitudinal mode at $\approx 2 - 3\%$ of critical. Further experimental tests were performed at Elandsrand Gold Mine (Constancon [1992]) in an attempt to determine an appropriate damping mechanism. A detailed discussion regarding the longitudinal damping estimates extracted from the experimental results is presented in Appendix G. These results indicate that the first mode is more highly damped than higher modes, a result which is inconsistent with a relative proportional viscous damping mechanism. A general proportional damping model[2] appears to characterise the longitudinal dissipation characteristics of the mine hoist rope adequately. This model is applied for convenience, and is not considered to represent the true nature of the damping mechanism. With regard to the lateral damping characteristics of a mine hoist rope, Mankowski[1986] presents dissipation factors extracted from a laboratory experiment. Based on Mankowski's dissipation factors, it appears

[1] A relative proportional damping mechanism considers the material dissipation characteristics to be distributed in a manner which is proportional to the stiffness properties of the rope.

[2] A general proportional damping mechanism considers the material dissipation characteristics to be distributed in a manner which is proportional to both the stiffness and mass properties of the rope.

that aerodynamic drag may represent a more significant lateral damping effect than the inherent properties of the hoist rope. This is discussed further in Appendix H. In the context of the stationary steady state analysis, a proportional lateral damping mechanism will be assumed, where the damping in the fundamental mode is of the order of 0.05% of critical.

4.2 The Linear *Datum* Solution

In order to pursue the strategy proposed, it is necessary to formulate the datum solution to provide a basis for the stability analysis, and the comparative study of the system tuning. In the absence of axial transport velocity and catenary curvature, the undamped non-linear equations of motion for the catenary, as developed in chapter 3, reduce to:

$$u_{,tt} = c^2 u_{,ss} + c\{v_{,s}v_{,ss} + w_{,s}w_{,ss}\} \tag{4.1}$$

$$v_{,tt} = \bar{c}v_{,ss} + c^2\{(u_{,s}v_{,s})_{,s} + \frac{3}{2}v_{,s}^2 v_{,ss} + \frac{1}{2}w_{,s}^2 v_{,ss} + v_{,s}w_{,s}w_{,ss}\} \tag{4.2}$$

$$w_{,tt} = \bar{c}w_{,ss} + c^2\{(u_{,s}w_{,s})_{,s} + \frac{3}{2}w_{,s}^2 w_{,ss} + \frac{1}{2}v_{,s}^2 w_{,ss} + w_{,s}v_{,s}v_{,ss}\} \tag{4.3}$$

where c, $\bar{c}$ represents the longitudinal and lateral wave speed respectively. The three dimensional motion of the catenary is described by the displacements $u(s,t)$, $v(s,t)$, $w(s,t)$, which represent the longitudinal, in-plane lateral and out-of-plane lateral motion respectively. In the absence of in-plane lateral excitation, a trivial solution is assumed for the in-plane lateral displacement, ie. $v(s,t) = 0$. Since the in-plane motion is assumed trivial, the in-plane equation of motion may be discarded at this stage. Thus the equations of motion describing the planar response of the catenary due to out-of-plane lateral and axial boundary excitation reduce to:

$$u_{,tt} = c^2 u_{,ss} + c\{w_{,s}w_{,ss}\} \tag{4.4}$$

$$w_{,tt} = \bar{c}w_{,ss} + c^2\{(u_{,s}w_{,s})_{,s} + \frac{3}{2}w_{,s}^2 w_{,ss}\} \tag{4.5}$$

The solution of equations (4.4),(4.5) leads to the definition of the non-linear planar steady state response of the system. A consistent non-linear analysis would address these equations by approximating the solution via a harmonic balance or alternative method. Although this was an attractive analytical route to follow, it is important to consider the significance of such complexity in terms of a practical industrial solution, and particularly in the context of defining a simple design criterion. It is for this reason, that a linearised solution to equations (4.4),(4.5) is sought, which reflects single valued response and provides a datum for approximating the degree of non-linear interaction which could be expected.

Primary external resonance of the catenary represents a principal consideration in the assessment of the mine hoist system. In general such a condition is unavoidable. However in these regions it would be advantageous to assess the system parameters, so that further non-linear coupling could be minimised. From a practical perspective it is accepted that mine hoist ropes will reflect dynamic behaviour, thus at this stage the knowledge of the steady state non-linear amplitude is of secondary importance with regard to the achievement of the best possible condition of tuning to minimise or avoid such behaviour.

Secondary conditions of resonance have not received attention in the context of the mine hoist system. Here the linear solution approximates a possible branch of the non-linear motion. Secondary resonance arises when this solution branch is unstable, and the response is attracted to an alternative dynamic state. In the context of this discussion, a linearised form of equations (4.4),(4.5) is proposed for the datum solution as:

$$u_{,tt} = c^2 u_{,ss} + c\{w_{,s}w_{,ss}\} \tag{4.6}$$

$$w_{,tt} = \bar{c}w_{,ss} \tag{4.7}$$

These equations reflect the coupling between the lateral and longitudinal motion, where the lateral steady state motion provides direct excitation to the

longitudinal system. Retaining the non-linear lateral coupling term in the longitudinal equation of motion is consistent with the ordering $uo(w^2)$. Conversely, the counter coupling of the longitudinal response on the lateral motion is discarded, since if $uo(w^2)$, then the quadratic term $(u_{,s}v_{,s})_{,s}\, o(w^3)$. This implies that the lateral motion is small, and hence excludes the condition of primary external resonance of the catenary. Away from regions of primary external resonance of the catenary, the cubic term $w_s^2 w_{ss}$ may be neglected. Thus the datum solution proposed is valid for identifying regions of secondary resonance, however due to the neglect of cubic terms, it is not valid close to a condition of primary external resonance. However, it is the boundary of stability which is sought, which may be close to, but not exactly tuned to a condition of primary external resonance. Since the solution essentially describes the lower branch of the response on either side of the resonant condition, it cannot predict regions of subcritical stability, where a higher amplitude stable solution branch may exist, which may be reached through initial conditions due to transient forces. The intention of the analysis is to identify regions where non-linear interaction is likely, and even under conditions of primary external resonance of the catenary, the datum solution will reflect the compliance of the longitudinal to lateral tuning, and it is proposed that the exponent of growth associated with the unstable datum solution in this region provides a comparative basis for assessment. Thus the stability analysis of the datum solution requires both the definition of the region of instability as well as the exponent of growth. This is a normal consequence of the stability technique chosen to examine the stability of the datum solution to small disturbances.

In conclusion, the datum solution is defined to provide a basis for a comparative assessment of the system tuning with regard to system parameters, and is not intended to represent the global non-linear steady state solution. Since the datum solution is valid in the absence of primary external resonance, regions of secondary resonance may be identified confidently. In light of the non-stationary nature of the system, an extensive study of the non-linear planar stationary motion would be counter productive, since a numerical simulation would ultimately be required. It is emphasised that the datum solution was primarily motivated to illustrate the existence of secondary resonance conditions, which are less obvious to a designer. It is expected that further research will refine the datum solution, to account for primary external resonance of the catenary. Appendix J presents a further discussion of the stationary steady state behaviour in the context of non-linear studies presented in the literature, and with regard to the existence of secondary and internal resonance conditions which are defined via the method of multiple scales. Appendices C,D,E present the closed form datum solution in the presence of general proportional damping, and axial and lateral out-of-plane boundary excitation at the winder drum, due to the first two harmonics of the Lebus groove excitation.

4.3 Stability of the *Datum* Solution

The steady state planar response, which is referred to as the datum solution, and represents the closed form continuous solution to equations (4.6),(4.7), is considered in the context of the non-linear equations (4.4),(4.5) of motion of the catenary. Variational equations of motion are constructed by considering small perturbations around the steady state datum solution. This is represented by:

$$\begin{aligned} u(s,t) &= \overline{u}(s,t) + u_D(s,t) \\ v(s,t) &= \overline{v}(s,t) \\ w(s,t) &= \overline{w}(s,t) + w_D(s,t) \end{aligned} \tag{4.8}$$

where $\overline{u}(s,t)$, $\overline{v}(s,t)$, $\overline{w}(s,t)$ represent small variations in the longitudinal, in-plane lateral and out-of-plane lateral motion with respect to the steady state datum solution $u_D(s,t)$, $v_D(s,t)$, $w_D(s,t)$. Substituting equations (4.8) into equations (4.4),(4.5), and considering *the homogeneous*[3] *component of the* linearised equations leads to[4]:

$$[1+\zeta\delta(s-l_1)+\eta(s-l_2)]\overline{u}_{,tt} = \mu\overline{u}_{,ss}+c^2\overline{u}_{,ss}+c^2\{w_{,s}\overline{w}_{,s}\}_{,s}[H(s)-H(s-l_1)] \tag{4.9}$$

$$\overline{v}_{,tt} = \mu_l\overline{v}_{,ss} + \bar{c}^2\overline{v}_{,ss} + c^2\{(\overline{v}_{,s}u_{,s})_{,s} + \frac{1}{2}(w_{,s}^2\overline{v}_{,s})_{,s}\} \tag{4.10}$$

$$\overline{w}_{,tt} = \mu_l\overline{w}_{,ss} + \bar{c}^2\overline{w}_{,ss} + c^2\{(\overline{w}_{,s}u_{,s})_{,s} + (w_{,s}\overline{u}_{,s})_{,s} + \frac{3}{2}(w_{,s}^2\overline{w}_{,s})_{,s}\} \tag{4.11}$$

$$\zeta = l/\rho AR^2, \quad \eta = M/\rho A$$

where l_1 represents the catenary length, *whilst* l_2 *represents the total cable* length. The longitudinal equation (4.9) is defined over the entire length of the

[3]Non-Homogeneous terms arise in the lateral variational equations. These terms represent a *residue related to* the neglect of the non-linear terms in the datum solution. In the presence of small steady state lateral motion ie. away from regions of primary external catenary resonance, the residue is considered small and is neglected.

[4]The boundary conditions at the sheave, and the skip are introduced via the use of the Dirac delta and Heaviside step functions. Thus the equations (4.9,4.10,4.11) represent the overall system equations *rather than just those* pertaining to the catenary.

rope $0 \leq s \leq l_2$, whilst the lateral equations (4.10),(4.11) are defined only over the catenary length $0 \leq s \leq l_1$.

The variational equations of motion may be reduced to ordinary differential form by applying a normal mode expansion for the continuous variables ie.

$$\overline{u} = \sum \phi_i(s) p_i(t)$$

$$\overline{v} = \sum \Phi_i(s) q_i(t)$$

$$\overline{w} = \sum \Phi_i(s) r_i(t) \tag{4.12}$$

where $\phi(s)$, $\Phi(s)$ represent the longitudinal and lateral eigen functions of the linear system. These are defined in Appendix C, D. Performing the orthogonalisation, leads to a set of coupled linear parametrically excited ordinary differential equations of the form:

$$[I]\{\ddot{y}\} + [2\zeta_n\omega_n]\{\dot{y}\} + \left[[\omega_n^2] + [A_d] + \sum_{n=1}^{4}[P(n\Omega t)]\right]\{y\} = 0 \tag{4.13}$$

where:

$$\{y\}^T = (p_i, q_i, r_i)$$

$$\sum_{n=1}^{4}[P(n\Omega t)] = \begin{bmatrix} 0 & 0 & U_{uw}(\Omega t, 2\Omega t) \\ 0 & V_{vv}(\Omega t, 2\Omega t, 3\Omega t, 4\Omega t) & 0 \\ W_{uw}(\Omega t, 2\Omega t) & 0 & W_{ww}(\Omega t, 2\Omega t, 3\Omega t, 4\Omega t) \end{bmatrix}$$

Where $[A_d]$ represents an initial stress matrix which represents the change in the variational natural frequencies due to a change in the average dynamic tension in the catenary. $[A_d]$ is defined in Appendix F.3.

The parametric coupling matrix $[P(n\Omega t)]$ and its constituent submatrices are defined in Appendix (F). It is pertinent to note that although modal truncation may occur with respect to the variational equations of motion, due to the application of the normal mode expansion, the datum solution is obtained

as a continuous solution and is not truncated. Periodic components in the parametric coupling matrix are generated up to the fourth harmonic of the Lebus coil cross-over frequency as a result of the first and second harmonic of the Lebus groove excitation. The parametric excitation matrix contains submatrices coupling the longitudinal and lateral modes. It is well established that regions of simple parametric resonance are dependent on the diagonal terms in the parametric excitation matrix (Hsu[1963]). Conversely regions of combination parametric resonance are dependent on the off diagonal terms. Thus simple parametric resonance does not arise with regard to the longitudinal modes alone. However, since the submatrices $[U_{uw}]$, $[W_{uw}]$ exist, regions of combination parametric resonance arise with respect to the longitudinal and lateral out-of-plane modes. Since the submatrices $[U_{uw}]$, $[W_{uw}]$ are not identical, it is possible that both additive and difference regions of combination resonance may arise, depending on the system parameters. Since the submatrices $[V_{vv}]$, $[W_{ww}]$ are symmetric, both simple and additive combination parametric resonance can occur with regard to the lateral in- and out-of-plane modes.

4.3.1 Stability of the Variational Equations

The criterion proposed as a design strategy for the mine hoist system amounts to an examination of the stability of the datum solution to small disturbances. The stability of the motion is dependent on the stability of equation (4.13). Linear systems with periodic coefficients have received much attention in the literature. A general discussion regarding parametric excitation is presented in Appendix K. A number of techniques can be applied to define the boundary of stability, for instance direct numerical integration combined with Floquet theory, perturbation techniques and the harmonic balance method. The first is numerically intensive, whilst the second is limited to the existence of small excitation and requires special attention for anomalous conditions of tuning (Hsu[1963]). Since a general approach is required which is capable of providing a stability chart regardless of the state of tuning, or the amplitude of excitation, a harmonic balance technique was applied. Takahashi[1981b] described an algorithm for determining regions of simple and combination parametric resonance of a parametrically excited system. This technique was applied in this study. A discussion of the method proposed by Takahashi[1981b] is presented in Appendix K.

The method is based on assuming an harmonic expansion for the response in

the form:

$$\{y(t)\} = e^{\lambda t}\{\frac{1}{2}\mathbf{b}_o + \sum_{n=1}^{\infty}(\mathbf{a}_n sin\ n\Omega t + \mathbf{b}_n cos\ n\Omega t)\} \tag{4.14}$$

Direct substitution of the assumed expansion (4.14) into equation (4.13), and applying the harmonic balance method leads to a relationship defining the response of the system in terms of the exponent λ, and the coefficients $\mathbf{b}_o, \mathbf{a}_n, \mathbf{b}_n$. Takahashi[1981b] demonstrated that this relationship could be formulated conveniently in matrix form. As a result, the method reduces to an eigenvalue extraction for the exponent λ. The stability of the system is thus dependent on $Re(\lambda) < 0$. In regions of instability, the exponent $Re(\lambda)$ reflects the initial exponential rate of growth of a disturbance away from the steady state solution. This exponent is extracted as a normal consequence of the solution, and is valuable in terms of the comparative study, since it is applied to assess the severity of a region of instability.

4.3.2 Experimental Validation

The method proposed to examine the stability of the steady state lateral motion of the catenary was confirmed experimentally. An experiment was conducted on a laboratory model of the mine hoist system. A photographic illustration of the experimental model is presented in figure 4.1. The model comprises of a guitar string, a pulley and a dead weight. The guitar string passes from a steel slider at one end, over a pulley wheel to a dead weight at the other end. An electro-dynamic shaker was applied to excite a single frequency sinusoidal lateral motion in the catenary[5]. The model was constructed so as to enable easy adjustment of the catenary length, and hence tuning of the lateral natural frequencies. It was found that the longitudinal system exhibited a single natural frequency in the test bandwidth, which could be tuned to some degree by changing the mass of the dead weight[6]. The free length between the pulley and dead weight was kept as short as possible to prevent lateral parametric excitation of this section[7]. The parameters of the model

[5]Since position feedback control was not applied to the shaker, the motion of the slider was monitored to ascertain that the system response did not affect the excitation wave form.

[6]The higher longitudinal modes fell well beyond the the test bandwidth of 0-100Hz. The first longitudinal mode occurred at approximately 20Hz, whilst the second occurred at $\approx$ 1.2 kHz.

[7]When a longer free length was accommodated, at certain tuning conditions, violent interactions between the catenary and free length section were evident. This presents an interesting condition of practical importance which is currently being considered.

Table 4.1: Laboratory model parameters

Parameter		1	2	3
Catenary Length	$l_c(m)$	0.479	0.485	0.790
Dead Weight	M (kg)	1.95	1.45	1.9
Pulley Inertia	J (kgm^2)	1.56×10^{-5}	1.56×10^{-5}	1.56×10^{-5}
Linear String Density	m (kg/m)	0.00745	0.00745	0.0268
Longitudinal Wave Speed	c (m/s)	1512.6	1512.6	845
Longitudinal Damping Factor	ζ (%)	0.2	0.2	0.8
Lateral Damping Factor	$\bar{\zeta}$ (%)	0.125	0.125	0.35

were accurately measured, and are tabulated in table 4.1. The most difficult parameter to measure was the longitudinal and lateral damping factor. These factors were approximated by impulsively exciting the system and determining the modal bandwidth of each mode.

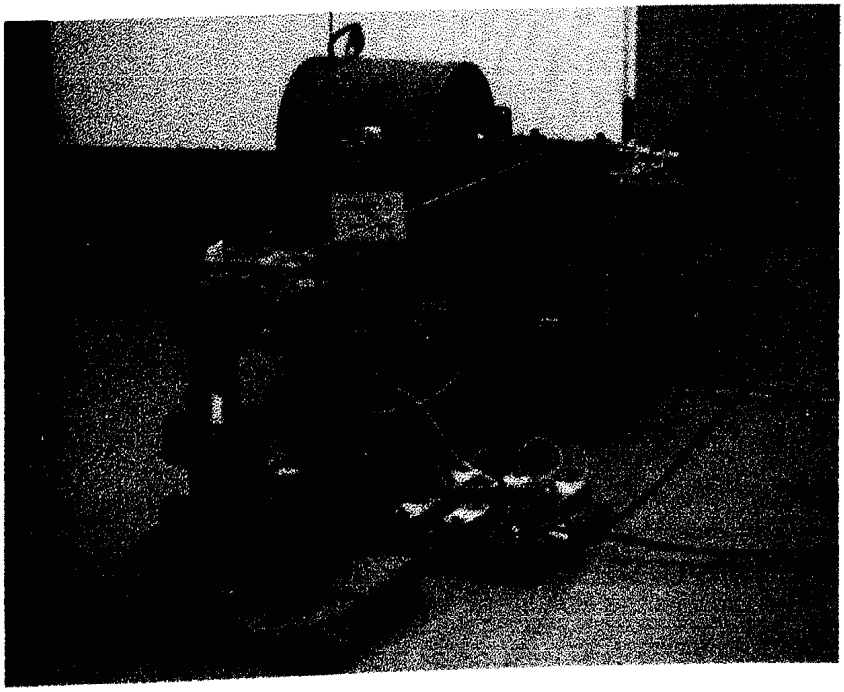


Figure 4.1: Laboratory model of the mine hoist system

The lateral amplitude of the excitation applied to the slider was monitored with an LVDT. The motion of the catenary in the lateral in- and out-of-plane direction was monitored with proximity probes. Since the range of the

Table 4.2: Tuning conditions of the laboratory model

Case	ω	$\overline{\omega}_1$	Resonance Condition
1	20.34 Hz	52.89 Hz	$\Omega \approx \overline{\omega}_1, \Omega \approx \overline{\omega}_2$ $\Omega \approx \omega + \overline{\omega}_1 \approx 73.23Hz$ $\Omega \approx \frac{1}{2}(\overline{\omega}_1 + \overline{\omega}_2) = \frac{1}{2}\overline{\omega}_3 \approx 79.33Hz$
2	22.5 Hz	45 Hz	$\Omega \approx \overline{\omega}_1, \Omega \approx \overline{\omega}_2$ $\Omega \approx \omega + \overline{\omega}_1 \approx 67.5Hz$ $\Omega \approx \frac{1}{2}(\overline{\omega}_1 + \overline{\omega}_2) \approx 67.5Hz$
3	16.55 Hz	16.69 Hz	$\Omega \approx \overline{\omega}_1, \Omega \approx \overline{\omega}_2, \Omega \approx \overline{\omega}_3$ $\Omega \approx \frac{1}{2}(\omega + \overline{\omega}_1) \approx \overline{\omega}_1 \approx 16.62Hz$ $\Omega \approx \omega + \overline{\omega}_1 \approx \overline{\omega}_2 \approx 33.24Hz$ $\Omega \approx \omega + \overline{\omega}_2 \approx \overline{\omega}_3 \approx 50Hz$

proximity probes was limited to $\pm 0.5mm$, they were positioned close to the pulley wheel where the lateral amplitudes remained small. The motion of the dead mass was monitored with a piezo crystal accelerometer. The transducer signals were analysed continuously by constructing the autospectra of each transducer signal on a Genrad 2515 analyser.

The purpose of the experiment was to confirm the existence of secondary regions of resonance related to combination parametric resonance of the out-of-plane lateral and longitudinal modes, as well as additive combination parametric resonance involving either the in-plane or out-of-plane lateral modes only. Three cases of system tuning were considered as presented in table 4.2, where Ω, ω, $\overline{\omega}_i$ represent the excitation frequency, and the longitudinal and lateral natural frequency respectively.

The first case represents a general state of tuning, where the combination resonance involving the longitudinal and first lateral mode is distinct from other combination resonances involving the lateral modes only. The second case considers the condition where a region of combination resonance involving the longitudinal and first lateral mode overlaps with the second region of combination resonance of the first and second lateral modes, as well as the second region of primary resonance of the third lateral mode etc. The third case considers the condition where the longitudinal and first lateral mode are closely tuned to one another. In this case, regions of combination parametric resonance occur simultaneously with conditions of primary external resonance of the lateral modes. The second and third cases coincide with a condition of internal resonance ie. $2\overline{\omega}_1 = \omega$, $\overline{\omega}_1 = \omega$, as defined by the perturbation analysis presented in Appendix J .

The boundary of stability of the planar steady state motion was determined experimentally by adjusting the excitation frequency, and then increasing the excitation amplitude until the response reflected a sudden growth in the motion. This condition was examined by viewing the signals from the proximity probes as a Lissajous plot on an oscilloscope. It was clearly evident that once a region of instability was entered, the steady state forced response was disrupted, indicating a change in the nature of the motion. In the first case, the boundary of stability associated with the longitudinal and lateral combination resonance resulted in unstable planar motion, which remained planar[8]. However, the combination resonance relating to the lateral modes only ie. $\Omega = \frac{1}{2}(\overline{\omega}_1 + \overline{\omega}_2) \approx \frac{1}{2}\overline{\omega}_3 \cdots$ was characterised by non-planar motion[9]. In regions close to primary external resonance of the lateral modes ie.$\Omega = \overline{\omega}_i$, the boundary of stability was characterised by a growth of the in-plane motion, leading to non-planar whirling motion.

With regard to the second and third case, the boundary of stability was characterised by planar and non-planar motion. With regard to the third case, it was found that since the natural frequency of the longitudinal mode was slightly lower than that of the first lateral mode, the left hand side of an unstable region of instability was characterised by a combination resonance involving the lateral and longitudinal modes; On this boundary, the planar steady state motion became unstable and initially remained planar. The right hand side of an unstable region was characterised by a growth of the in-plane motion immediately leading to non-planar motion.

In all cases, for a large enough amplitude, violent non-planar motion was observed. It was also evident that once this motion had evolved, it was difficult to detune the resonance by simply increasing or decreasing the excitation frequency.

The stability chart of the steady state motion constructed from the experimental model was compared with the stability chart obtained via the analytical technique proposed in this chapter. The variational equations were truncated to account for a single longitudinal mode, and three in and out-of-plane lateral modes. The harmonic balance method was applied to determine these regions, where a five term harmonic expansion was employed. The accuracy of the stability chart was verified via direct numerical simulation of the variational equations. The experimental and analytical stability charts pertaining to the

[8]On the boundary of stability, the autospectra of the longitudinal and lateral response indicated dominant response close to the natural frequencies related to the longitudinal and first lateral modes respectively.

[9]The autospectrum of the lateral motion indicated multi-modal response in the lateral modes.

laboratory model are presented in figure 4.2 for the three cases considered. The experimental results are indicated in figure 4.2 by a +, whilst shaded regions indicate the analytically determined regions.

Figure 4.3 illustrates typical stable and unstable motion observed during the experiment. The photographs were obtained by strobing the catenary at a slightly lower frequency than the excitation frequency, and using a time exposure to photograph the motion. These photographic slides illustrate the stable/unstable motion of the catenary on the boundary of stability for the third case of tuning. In this case, the excitation frequency and amplitude were such that the system passed from stable to unstable motion through the left hand boundary of the second and third region of primary external resonance.

Generally, the experimentally determined boundary of stability correlates well with the analytically determined regions of instability. Since the datum solution is representative of the steady state motion away from conditions of primary external resonance, the boundary of stability associated with regions close to primary external resonance are approximate. However, since the condition of primary external resonance is contained within the region of instability, and since the lateral damping factor is small and consequently the modal bandwidth is small, reasonable accuracy was achieved even for this condition. With regard to the first case of tuning, the second region of combination parametric resonance related to the lateral modes ie. $\Omega = \frac{1}{2}(\overline{\omega}_1 + \overline{\omega}_2) = \frac{1}{2}\overline{\omega}_3$ indicates stiffening behaviour, as predicted by the analytical solution. It was difficult to excite this region, since more precise tuning was required, and consequently it was not easy to tune the system to a condition of neutral stability and thus identify the boundary precisely. It is also important to recognise that although the laboratory model is representative of the mine hoist system, the analytical technique models a slider at the pulley end. It is proposed that this contributes to the higher degree of stiffening predicted analytically for the region, in comparison to the experimental results; also as discussed in chapter 5, the application of a normal mode technique contributes to stiffer behaviour.

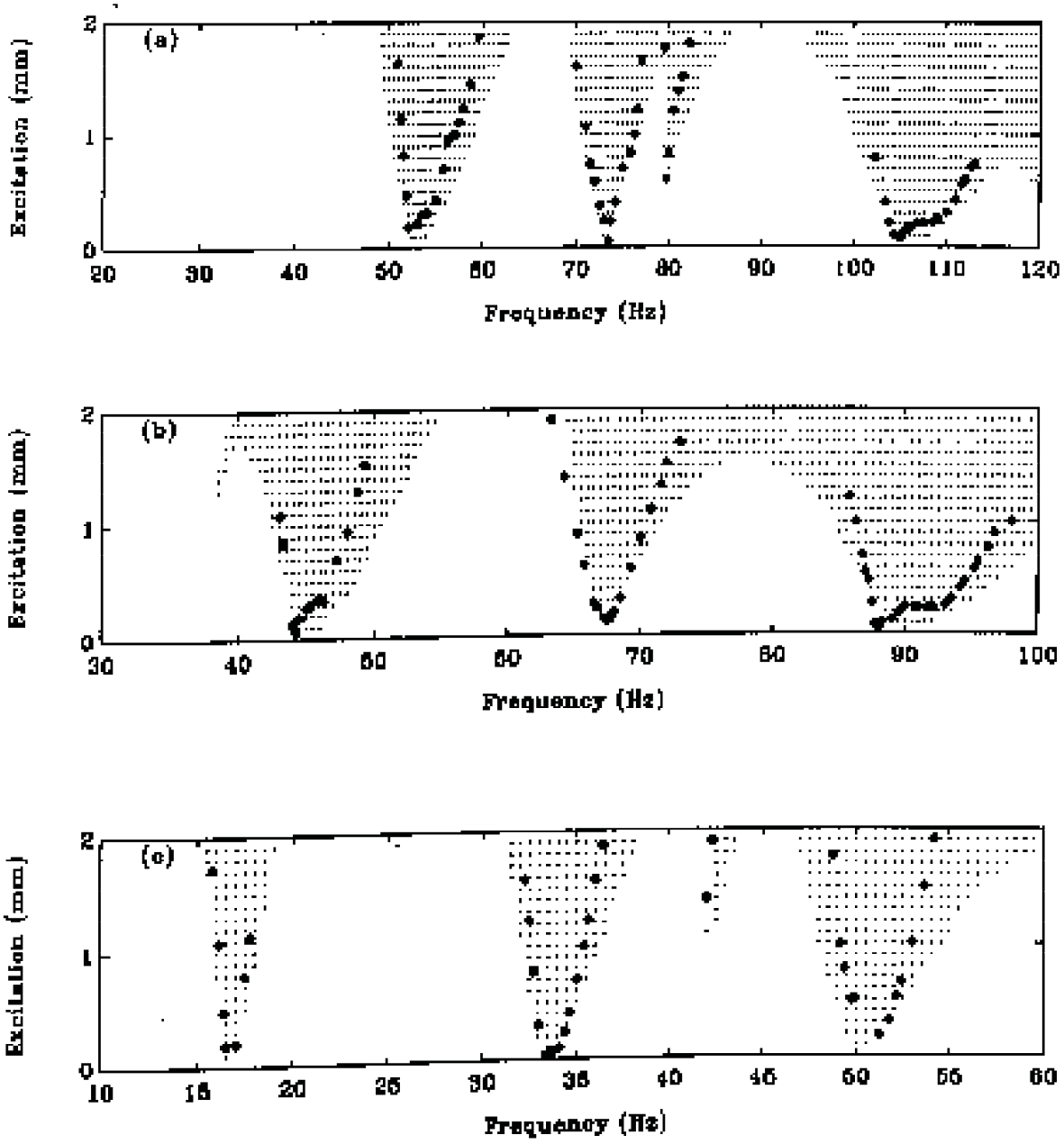


Figure 4.2: Stability chart of the laboratory model
a) Case 1.
b) Case 2.
c) Case 3.
\+ Experimental

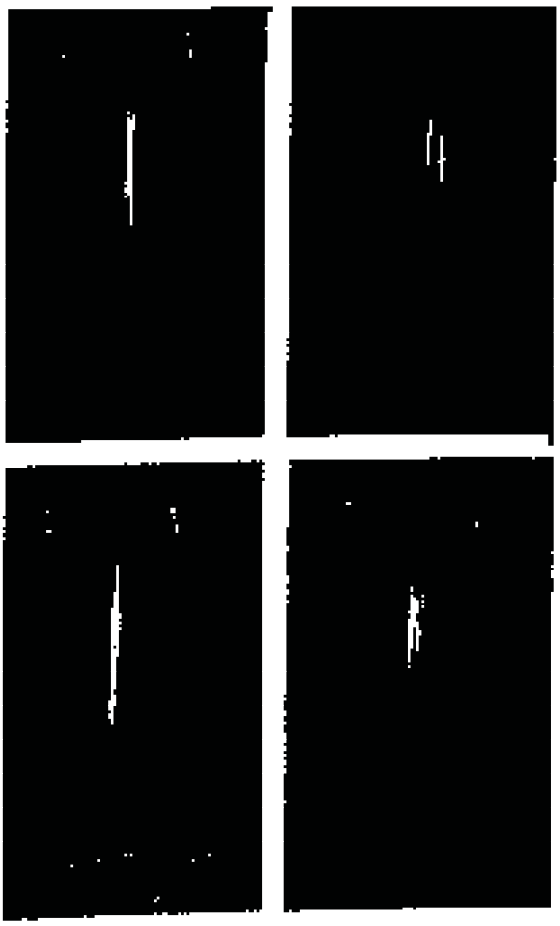


Figure 4.3: Stable/unstable catenary motion - Case 3.

a) Stable motion $\Omega \approx \varpi_2$ b) Unstable motion $\Omega \approx \varpi_2$
c) Stable motion $\Omega \approx \varpi_3$ d) Unstable motion $\Omega \approx \varpi_3$

4.4 The Kloof Mine Hoist System

The stability analysis developed in this chapter is applied to examine the Kloof Mine hoist system. As discussed in chapter 1, this system experienced severe rope whip during the ascending cycle. Dimitriou and Whillier[1973] analysed this system by examining the quasi-static description of the system characteristics. Although this is a useful approach to identify potential regions of primary external resonance, it fails to account for the physical system parameters such as damping, the level of excitation and the potential influence of lateral to longitudinal tuning. The Kloof Mine Hoist system parameters applied in the analysis are presented in table 4.4. Figure 4.4(a,b) presents the linear dynamic characteristics of the system during the descending and ascending cycle respectively. The horizontal lines in figure 4.4(a,b) represent the first and second harmonic of the Lebus excitation frequencies, at a constant nominal winding speed of 15 m/s[10]. The vertical lines reflect the layer change-over locations. It is evident in figure 4.4(b) that during the ascending cycle the second lateral mode of the catenary is resonant at approximately 700m. This occurs simultaneously with the second longitudinal mode. Prior to this condition at approximately 900m, the fourth longitudinal mode is tuned to twice the second lateral catenary mode and hence a condition of internal resonance arises.

The stability chart of the steady state solution was constructed as a function of shaft depth and the nominal winding velocity, whilst the excitation amplitude at the winder drum, as determined from the Lebus groove geometry[11] was held constant. The purpose of this chart is to reflect regions of avoidance of likely non-linear interaction, and hence to determine a viable winding speed for the given system parameters. Only two regions of instability were evident on the ascending cycle, and these were related to direct external resonance of the third and second lateral catenary modes, at the beginning and end of the wind respectively. The eigenvalue exponents associated with these regions did not reflect any local maximum, or special condition of tuning between the lateral and longitudinal system. Figure 4.5 illustrates the stability chart for the ascending cycle[12]. The region of instability is related to primary external resonance of the second and fourth catenary modes. Although the steady state or datum solution accounts for conditions away from primary external

[10]The nominal winding speed reflects the drum surface speed, consequently the rope speed increases as the number of rope layers increase.

[11]Appendix A presents the definition and calculation of the Lebus groove excitations.

[12]The shaded region of the chart represents an unstable solution, where the eigenvalue of exponent λ is greater than zero. The contours on the shaded region represent the magnitude of the exponent λ. The maximum exponent is 110, whilst the countour lines represent an exponent of 0.01,.1,1,10,50,100.

resonance of the catenary, it is clearly evident from the eigenvalue plot that a significant region of interaction is predicted close to 15m/s, which spans approximately 100 m from 650m-750m. This region is characterised by the interaction of two conditions of resonance. The solid lines on this figure reflect various conditions of resonance. The solid line represented by (b) reflects the additive combination resonance of the second catenary and second longitudinal mode. Even though the second catenary mode is resonant away from this winding speed, the eigenvalue plot reflects that the severity of the tuning drops.

In order to accentuate regions of secondary resonance, a similar stability chart was constructed for the ascending and descending cycles, where the winding velocity was maintained at 15 m/s, whilst the amplitude of the excitation and hence of the steady state motion was increased proportionately. These charts are presented in figures 4.6,4.7 respectively. In these charts the nominal Lebus groove excitation is amplified by a factor of ϵ. Secondary regions of resonance are evident in these figures. However substantial steady state excitation would be required to activate such regions. With regard to the ascending wind, presented in figure 4.6, the region at 250m is related to a condition of parametric combination resonance of the first lateral and longitudinal modes, which tune to the first harmonic of the Lebus excitation frequency. The region to the right of the primary resonance ($\approx 900m$) region is related to resonance of the fourth longitudinal mode, combined with the internal resonance between the fourth longitudinal and second lateral modes. The descending cycle exhibits similar regions of secondary resonance. The two most significant regions are related to primary external resonance of the third lateral catenary mode ($\approx$ 300m) and of the second lateral mode towards the end of the wind ($\approx$ 1700m). The latter condition is larger and more important as it spans a greater section of the wind. This is confirmed by the simulation results presented in Chapter 5.

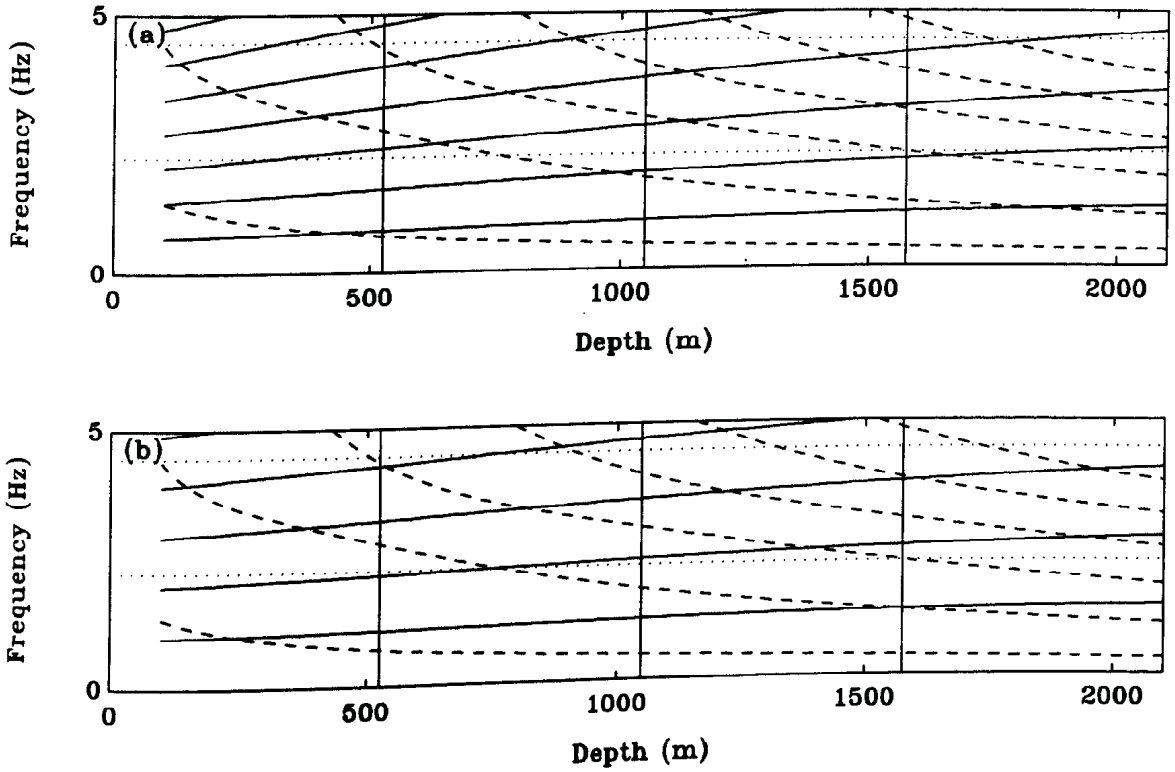


Figure 4.4: .Kloof Mine: Linear dynamic characteristics.

a) Descending cycle b) Ascending cycle

... Lebus groove excitation frequency

– – Longitudinal natural frequencies

—— Lateral natural frequencies

Table 4.3: Kloof Mine - System parameters

J	Sheave Inertia.	15200 kgm^2
M	Skip Mass.	7920 kg
M0	Skip Pay-load.	9664 kg
m	Linear Rope density.	8.4 kg/m
V	Nominal Winding Speed.	15 m/s
De	Depth of wind.	2100m
Lc	Catenary Length.	74.95 m
E	Effective Youngs Modulus of the rope.	$1.1E^{11}$
Ax	Effective steel area of the rope.	$0.001028m^2$
β	Cross over arc.	0.2 rad
Dd	Drum Diameter.	4.28 m
Ds	Sheave Diameter.	4.26 m
Dr	Rope Diameter.	0.048 m
μ_a	General proportional damping parameter	0.159
$\mu_b(s_2)$	General proportional damping parameter	$10.49s_2$
ζ_1	Lateral proportional modal damping ratio	0.05%

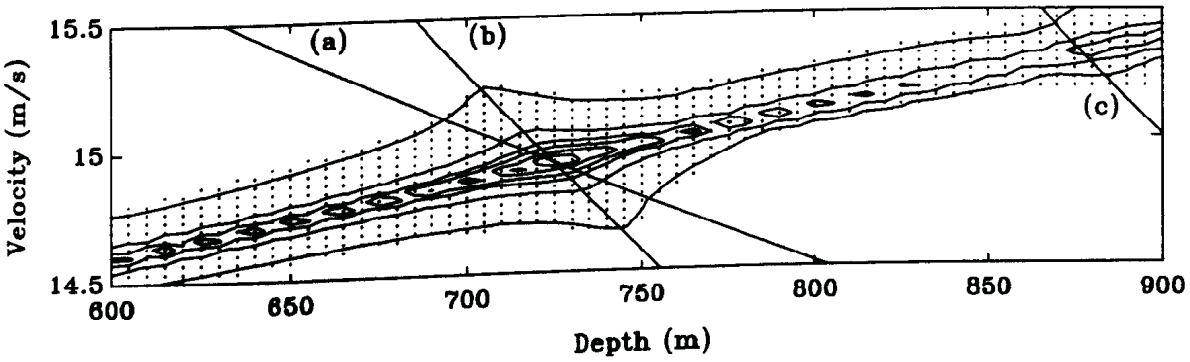


Figure 4.5: Stability chart of the steady state datum solution - Ascending

a) $2\Omega_{Lebus} = w_2 + \overline{\omega}_2$
b) $\Omega_{Lebus} = \overline{\omega}_2$
c) $\Omega_{Lebus} = \overline{\omega}_4$

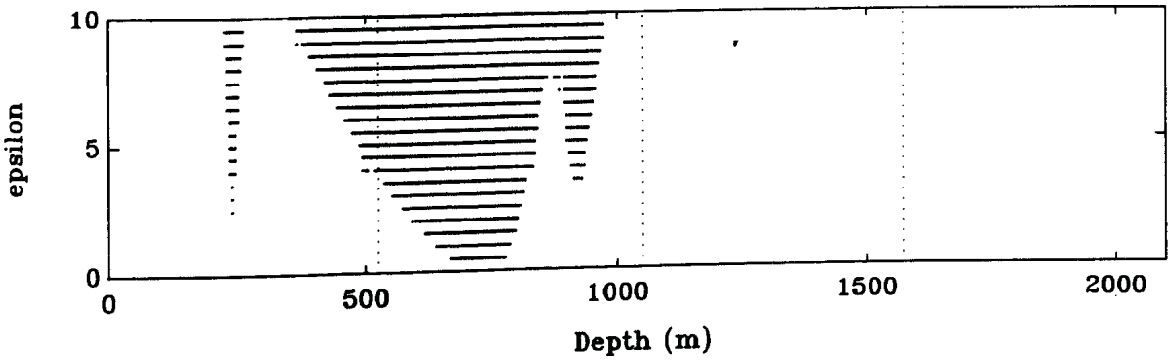


Figure 4.6: Stability chart of the steady state datum solution - Ascending Increasing amplitude of excitation ϵ, $\zeta_1 = 0.05\%$

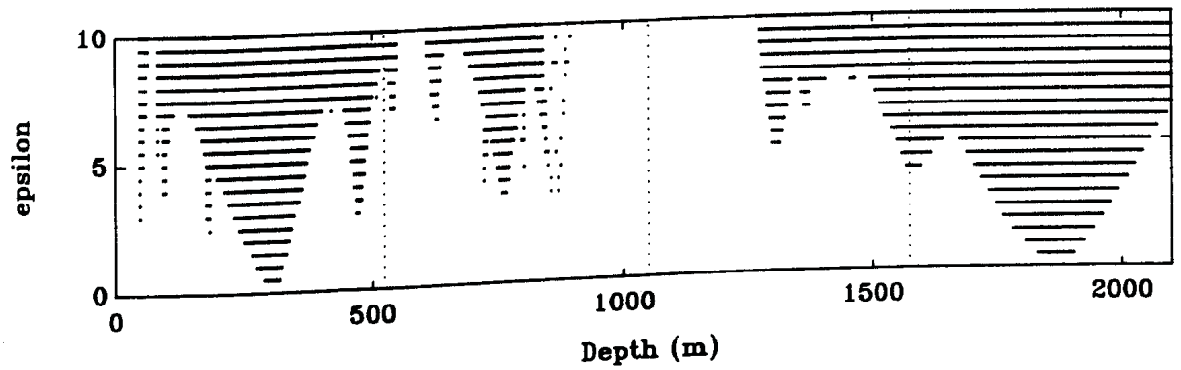


Figure 4.7: Stability chart of the steady state datum solution - Descending Increasing amplitude of excitation ϵ, $\zeta_1 = 0.05\%$

4.5 Conclusion

The purpose of the steady state analysis was to identify regions where non-linear interaction is likely. The analysis was validated experimentally and then applied to examine the Kloof Mine hoist system characteristics. Satisfactory correlation was achieved with respect to the laboratory experiment. In the context of a hoisting system, the analysis would provide a preliminary assessment of the hoist characteristics. It is important to emphasise that the stationary steady state analysis was intended to compliment the linear approach proposed by Dimitriou and Whillier[1973]. It is limited in that it does not account for the non-stationary behaviour of the system, nor does it account for the transient excitation introduced during the acceleration/deceleration phases or during layer change-overs. In effect, the mine hoist system does not achieve steady state; the effect of the winding velocity is to attenuate and delay the resonant condition. The transient excitations introduced at the layer change, may also significantly influence the dynamic state of the system; the location of layer changes is pertinent, since the phase of the out-of-plane lateral excitation changes by 180^o after a layer change. This mechanism can be used to advantage to precipitate resonant amplitudes from developing further. In terms of the stationary analysis of the Kloof Mine hoist system, the analysis serves to confirm to some degree the observation of Dimitriou and Whillier that the lateral motion may induce significant longitudinal interaction at approximately 700m. It is evident from the stability (figure 4.5) plot that this occurs in the vicinity of 15m/s. Hopefully such information would draw attention to this condition of tuning, and such a condition would be avoided. For realistic stationary excitation levels calculated from the drum geometry, significant regions of secondary resonance as observed in the laboratory experiment, do not arise on the Kloof mine hoist system. However, at substantially larger excitation levels such regions may be entered, as is evident in figures 4.6, 4.7. During a winding cycle, the dynamic response never reaches steady state, and consequently the residual response due to the non-stationary nature of the system may activate regions of secondary resonance. In light of these additional features of the system, a numerical simulation is necessary as a final validation of the system design. Such a simulation is presented in the following chapter.

Chapter 5

Nonlinear Numerical Simulation

Chapter 4 presented a stability analysis of the steady state out-of-plane datum solution. The stability of this motion was investigated as a criterion to identify system parameters which reduced the nonlinear coupling between the lateral and longitudinal motion. The analysis confirmed the existence of simple and additive combination parametric resonances of the lateral modes, as well as the possibility of parametric resonance involving additive and difference combinations of the longitudinal and lateral modes. A further discussion regarding the steady state motion is presented in Appendix J, where the existence of these regions of secondary resonance is confirmed by applying the method of multiple time scales to examine the nonlinear equations of motion directly. The perturbation analysis also identifies conditions of tuning which lead to internal resonance. Although an appreciation of the steady state stability of the system may be useful for identifying regions of potential nonlinear interaction, the system is non-stationary, and steady state motion is never attained. In addition the Lebus excitation at the drum was idealised in the stability analysis as a two term Fourier expansion of the groove profile. In reality the Lebus groove profile induces strong pulses at each coil cross-over. Thus modelling the geometry of the cross-over region accurately is essential. For this reason, a numerical simulation capable of approximating the real time response of the system is developed. Since such an analysis is intended to simulate the behaviour of the system as realistically as possible, nonlinear terms consistent with the strain definition, as well as cable curvature and cable transport velocity are included in the analysis.

This chapter progresses through three phases. Firstly the nonlinear partial differential equations of motion as derived in chapter 3 are considered. Thereafter, a numerical simulation of these equations is developed. In the early stages of this study, the normal mode method was applied to transform the partial differential equations of motion to ordinary differential form. An extensive simulation based on this approach was developed. The numerical simulation failed to correlate with measurements extracted from the laboratory model of the system. This exercise demonstrated the limitations of a nonlinear normal mode approach, and resulted in the development of a quasi-static model for the catenary section. Finally a nonlinear simulation of the Kloof Mine hoist system, based on a quasi-static model which includes catenary curvature and transport velocity, is presented. The numerical simulation predicts dynamic interactions on the up-wind, leading to rope whip, as observed by Dimitriou and Whillier[1973], whilst negligible interaction occurs on the down-wind.

5.1 Nonlinear Equations of Motion

5.1.1 Simplifications Applied in the Modelling Process

The nonlinear equations of motion were developed by applying Hamilton's principle. In developing these equations, the Lagrangian strain in the axial direction of the rope was defined as:[1]

$$\epsilon = u_s - \kappa v + \frac{1}{2}(v_s^2 + w_s^2)$$

Since the catenary curvature is small, the catenary is treated as a symmetric horizontally supported cable with constant curvature, where the equilibrium curvature is defined as:

$$\kappa = \frac{mgcos(\theta)}{H}$$

where θ refers to the angle of inclination of the catenary and H is the equilibrium tension. Typically the curvature will vary between $1 \times 10^{-4} < \kappa < 1 \times 10^{-3}$.

[1]Since the correct expression for the strain is: $\epsilon = u_s - \kappa v + \frac{1}{2}((u_s - \kappa v)^2 + w_s^2 + (v_s + \kappa u)^2)$, $uO(v^2), O(w^2), \kappa O(u)$, where u, v, w represent axial, lateral in-plane and out-of-plane motion respectively.